LONGITUDINAL BUNCH SHAPE DIAGNOSTICS WITH COHERENT RADIATION AND A TRANSVERSE DEFLECTING CAVITY AT TTF2

L. Fröhlich, O. Grimm*, K. Klose, M. Nagl, O. Peters, J. Rossbach, H. Schlarb
DESY, Hamburg, Germany
M. Ross, T.J. Smith, D. McCormick, P.J. Emma
SLAC, Menlo Park, USA

Abstract

At the DESY TTF2 linear accelerator three special techniques to characterize the longitudinal charge distribution of the electron bunches that drive the free-electron laser are currently under study: electro-optical sampling, far-infrared spectral analysis of coherent radiation and the use of a transverse deflecting cavity to streak the bunch. The principles and implementations of the latter two are described in this paper. Details on electro-optical sampling can be found in [1].

INTRODUCTION

The VUV-FEL at DESY, Hamburg, will require novel techniques to characterize the longitudinal charge distribution of the electron bunches that drive the free-electron laser. Conventional methods, e.g. streak cameras, are inadequate due to both the short bunch lengths of the linac and the high sensitivity of the lasing process to spikes in the charge distribution which therefore need to be known with high resolution. Three techniques are currently investigated at TTF2:

- Analysis of the far-infrared spectrum of synchrotron, transition, diffraction and undulator radiation. At wavelengths comparable to or longer than the bunch length or a particular longitudinal feature of the bunch, the spectrum will be modified by coherent effects.
- Streaking the bunch with a transverse deflecting RF structure. The longitudinal profile is converted into transverse space and thus becomes observable with a camera on, e.g., an optical transition radiation screen.
- Measuring the electric field strength through electro-optical sampling. The interaction of a laser pulse much shorter than the electron bunch with the bunch electric field in a nonlinear crystal gives rise to a detectable effect on the laser polarization (see [1] for details).

The first technique, working in the frequency domain, has no requirements on timing or triggering precision, but the bunch shape is accessible only through an ambiguous inversion process, whereas the latter two techniques are directly sensitive to the longitudinal charge distribution and need precise timing.

* Corresponding author. E-Mail: oliver.grimm@desy.de

A new method, consisting essentially of the generation of an optical replica of the longitudinal bunch shape and then a two-dimensional measurement of this replica in frequency and time domain simultaneously, has recently been proposed in [2].

FAR-INFRARED ANALYSIS OF COHERENT RADIATION

Analysis principle

The bunch shape is imprinted on the radiation spectrum $\mathrm{d}U/\mathrm{d}\lambda$ through the form factor $F(\lambda)$,

$$\frac{\mathrm{d}U}{\mathrm{d}\lambda} = \left(\frac{\mathrm{d}U}{\mathrm{d}\lambda}\right)_0 \left(N + N(N-1)\left|F(\lambda)\right|^2\right), \qquad (1)$$

where $(\mathrm{d}U/\mathrm{d}\lambda)_0$ is the emission spectrum of one single electron, N is the total number of electrons and the form factor is the Fourier transform of the normalized longitudinal charge distribution $S(z)$ ($\int_{-\infty}^{\infty} S(z)\,\mathrm{d}z = 1$),

$$F(\lambda) = \int_{-\infty}^{\infty} S(z) \exp\left(\frac{-2\pi \mathrm{i}}{\lambda} z\right) \mathrm{d}z. \qquad (2)$$

The basic assumption in the derivation of these equations is that each electron generates a time-dependent electric field at a given position that is the same for all electrons except a time delay (corresponding to a spacial distance), i.e. $\vec{E}_i(t) = \vec{E}_0(t + \Delta t_i)$.[1]

Measurement of the total spectrum and knowledge of the number of electrons and the single-electron spectrum then gives access to the modulus of the form factor. The final step of inverse Fourier transforming this to arrive at the bunch shape requires knowledge of the phase of the Fourier transform. The phase is not completely arbitrary but also not unambiguously determined by the modulus [3], therefore a full bunch shape reconstruction is impossible. The technique of Kramers-Kronig analysis, however, allows to retrieve some of the missing phase information. If one writes for the complex form factor $F(\omega) = |F(\omega)| \exp(\mathrm{i}\psi(\omega))$, with ω the angular frequency, then

$$\psi(\omega) = -\frac{2\omega}{\pi} \int_0^{\infty} \frac{\ln(|F(x)|/|F(\omega)|)}{x^2 - \omega^2} \mathrm{d}x \qquad (3)$$

[1] This limits the allowable transverse size: particles offset from the centre will contribute with a time delay just as particles further behind, thus washing out spacial structures. Additionally, the emission spectrum generally changes with angle, also limiting the tolerable transverse size.

is the minimum phase value consistent with the measured modulus [4]. Application of the Kramers-Kronig analysis requires knowledge of the form factor modulus from zero to infinite frequency, thus an extrapolation of measured data. Some extrapolation has been suggested in [4], but experiences from the first run of TTF show that the results are quite sensitive to these extrapolations and detailed studies of their effects are necessary [5].

Currently, the opposite way is pursued: simulations are performed to calculate the spectrum for some expected bunch shapes and then compared to the measurements. An example, referring to the synchrotron radiation beamline described in the next section, where the actual magnetic field of the fourth BC2 magnet, the vacuum chamber cut-off (see [6]) and the form factor for three bunch shapes have been taken into account is shown in Fig. 1. The spectrum is averaged over the clear aperture of the window. A parametrization for the two sharply peaked shapes is given in [7]. Not yet included is the transmission characteristic of the beamline and the frequency response of the pyroelectric detectors. Interference with radiation from the third magnet will modify the spectrum, but also requires further understanding of the beamline optics and has been neglected here.

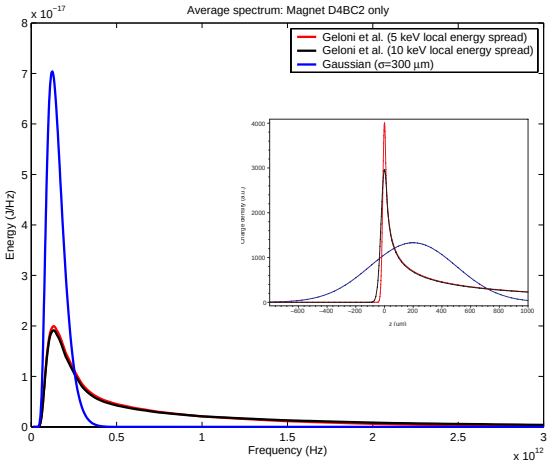

Figure 1: Simulated spectrum after (1). Included are the form factor for the bunch shapes shown in the inset, the chamber cut-off and the window transmission.

Precise knowledge of all spectral modifications by the vacuum chamber, beamline mirrors and apertures, interferometer and detectors is required to extract the form factor. One experimental approach to determine these factors is to use a blackbody source (having a known emission spectrum) at the beginning of the beamline and then to measure the spectrum with the interferometer as used for bunch length determination. This way, all effects are taken into account correctly except the coupling between source and beamline. The intensity in the far-infrared of such a source is very low, but might be sufficient if a sensitive liquid Helium cooled bolometer is used. The other, calculational approach is to use optical simulation software to assess the transmission characteristics of the beamline and the interferometer and to calculate vacuum chamber cut-off and detector response from detailed considerations of their geometries and configurations. A combination of all techniques appears to be necessary to get to a sufficiently precise answer.

An interesting alternative would be a synchrotron radiation source that is guaranteed to emit only incoherent radiation at the frequencies of interest. This requirement would be fulfilled by long, smooth bunches, but it is currently not clear how this could be assured at TTF2. Even small bunch structures would easily dominate due to coherent emission.

Synchrotron radiation beamline at TTF2

A beamline to guide both far-infrared (50–3000 µm) and visible synchrotron radiation from the first bunch compressor (BC2) of the TTF2 linear accelerator to a diagnostic station outside of the controlled area at some 10 m distance has recently been constructed [8]. It will allow a direct comparison between streak camera and far-infrared measurements for features on length scales above some 100 µm (the streak camera resolution). Later, infrared techniques extending to shorter wavelengths, i.e. to shorter bunch lengths, will also be used further downstream the accelerator, employing synchrotron, transition and undulator radiation.

The principle design of the beamline relies on simple optics: a paraboloid mirror close to the synchrotron radiation viewport transforms radiation originating from an arc of about 7 cm length in the source region at some 81 cm distance into a nearly parallel beam which is then transported by large flat mirrors through Aluminium pipes to the experimental station. The beamline including the interferometer is flushed with dry Nitrogen to reduce the strong absorption of water vapour in the far-infrared. It is already partly prepared for later evacuation to fore-vacuum in case the absorption needs to be reduced further. A crystalline Quartz window (z-cut, clear aperture ⌀60 mm, 4.8 mm thick) is used as viewport.

Outcoupling port The synchrotron port at the fourth BC2 magnet (D4BC2) is at 18° relative to the beam axis, seeing approximately the first 2.5° of the beam trajectory arc. With a nominal bending radius of about 1.6 m at 130 MeV, this corresponds to an arc length of 7 cm. A photo of the port is shown in Fig. 2, a sketch of the geometry in Fig. 3.

The radiation is emitted along the arc into a cone of typical half-opening angle of 2.4° (42 mrad) at 250 µm and of 0.2° (3.5 mrad) at 500 nm. In the vertical the radiation beam is restricted by the vacuum chamber height of 16 mm, in the horizontal by the 60 mm diameter window. To transport this beam over some 10 m distance requires focusing of the infrared radiation soon after the chamber window

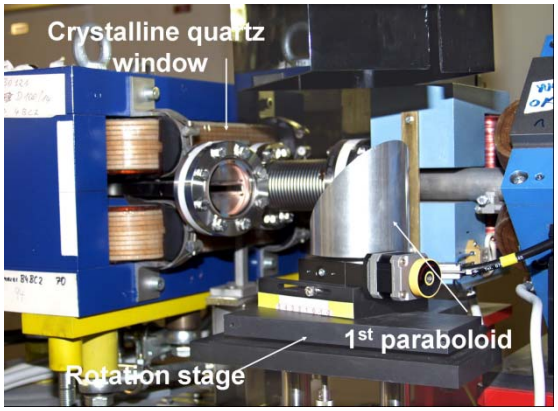

Figure 2: Outcoupling port of the beamline.

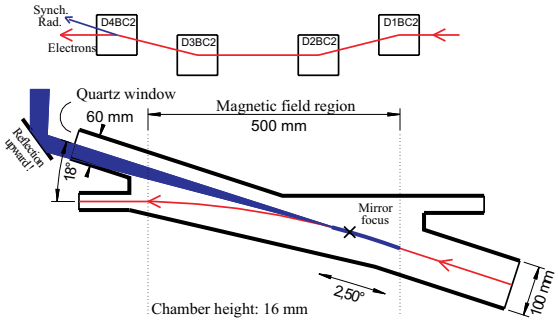

Figure 3: BC2 layout and D4BC2 vacuum chamber.

to limit the necessary mirror sizes. To this end, a 90° off-axis paraboloid mirror is installed after the window, reflecting the parallelized beam upwards to the tunnel roof. The paraboloid is machined from Aluminium, has a projected diameter of 100 mm and 810 mm focal length.

Depending on the bunch compressor settings, the electron beam can enter the dipole chamber at any position allowed by its 100 mm width. The mirror can be rotated around its vertical axis, such that the focal point follows the emission region of the synchrotron radiation. The rotation plane is aligned with the nominal electron beam plane. The focusing is not very sensitive to the exact longitudinal position, so that no translation of the mirror in this axis is necessary.

Transport line The approximately parallel beam from the paraboloid is reflected by a flat mirror under the tunnel roof straight out to further flat mirrors in the diagnostic container that feed the radiation into the interferometer or the streak camera. For the latter, narrow wavelength filters are used to avoid resolution loss due to dispersion in the window. The beam travels within large Aluminium pipes of 250 mm diameter (200 mm over a short section through the radiation protection wall) to avoid additional diffraction losses. Nitrogen is flushed from the diagnostic station into the tunnel at flow rates below 1 l/s, so that effluence into the tunnel is of no security concern.

Interferometer A polarizing Martin-Puplett interferometer[2] is used to analyze the spectrum of the far-infrared radiation. The wire grids are wound from 10 µm gold-plated Tungsten wire with 30 µm spacing, so that the interferometer works at wavelengths longer than about 60 µm. The clear aperture of the device is about 10 cm diameter. Currently, DTGS pyroelectric detectors are used, a liquid Helium cooled bolometer will also be available for the next TTF2 run. Details of the device can be found in [9, Chapter 7].

Compared to a Michelson interferometer, this type has the advantage of an almost perfect beam splitter characteristic for wavelengths longer than about twice the wire spacing and full transmission of the incoming radiation to the detectors (whereas on average half is reflected back to the source with a Michelson device).

First results

During the first run of TTF2 in May/June 2004, the infrared beamline was commissioned and first interferograms were taken. Fig. 4 shows one example. Clearly visible is one advantage of the Martin-Puplett interferometer: it allows suppression of radiation intensity fluctuations by normalizing the detector signals to the total intensity, i.e. their sum. Such fluctuations were strong during this startup phase.

The interferogram shows a small secondary signal at about 67 ps delay, coming from reflections within the 4.8 mm thick Quartz window, also reflected in the spectrum by the interference structure. The spectral shape shows agreement on a broad scale with the first simulations (see Fig. 1), but more detailed understanding of transmission and detector effects is necessary to extract quantitative information.

TRANSVERSE DEFLECTING CAVITY

LOLA[3] is a disk-loaded waveguide structure with constant impedance, using the TM 11 hybrid mode. It was originally build as a separator for secondary particles with the same momentum but different mass, and is used now as a transverse deflector to streak electron bunches.

The main parameters of the structure are: length 3.66 m, iris aperture 44.88 mm, peak deflecting voltage 26 MV (at 20 MW), frequency 2856 MHz, filling time 645 ns (quality factor 12100). The latter characteristic allows to streak only a few bunches from the TTF2 bunch train, working in quasi parasitic-mode. Because of the constant impedance, the transverse deflecting electric field is decreasing along the structure. The phase shift per cell (35 mm length) is 120°. A photograph of the structure installed in the TTF2 tunnel is shown in Fig. 5.

[2] Build by RWTH Aachen.

[3] The name comes from its designers: Greg **LO**ew, Rudy **L**arsen and Otto **A**ltenmueller. It was built at SLAC 1968.

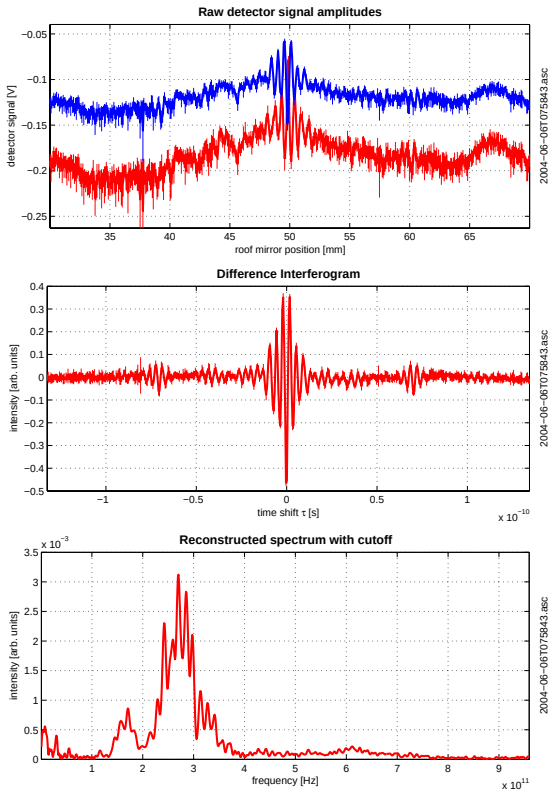

Figure 4: Measured raw (top) and normalized difference (middle) interferogram and the reconstructed spectrum (bottom) from the first run of TTF2 in May/June 2004.

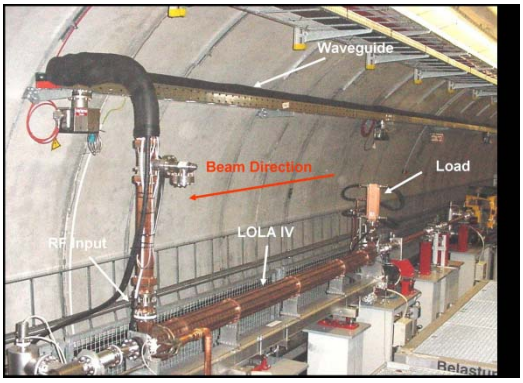

Figure 5: Photograph showing LOLA in the TTF2 tunnel.

Analysis

A particle within a bunch with position z relative to some origin will, after traversing the deflecting structure, have an offset $\Delta y(z)$ on a screen given by

$$\Delta y(z) = \frac{eV_0}{E_0}\sqrt{\beta_c\beta_p}\sin\Delta\psi_y\left(\frac{2\pi z}{\lambda}\cos\varphi + \sin\varphi\right). \quad (4)$$

Here, β_c and β_p are the beta function values at the cavity and at the screen, respectively, $\Delta\psi_y$ the beta function phase advance between them, V_0 the peak deflecting voltage and λ the wavelength of the structure, E_0 the electron energy and φ the phase angle between RF zero crossing and the bunch origin [10]. The observed spot size on the screen σ_y is related to the bunch length σ_z through (see Fig. 6)

$$\sigma_y = \sqrt{\sigma_{y,0}^2 + \sigma_z^2\beta_c\beta_p\left(\frac{2\pi eV_0}{\lambda E_0}\sin\Delta\psi_y\cos\varphi\right)^2}, \quad (5)$$

where $\sigma_{y,0}$ is the bunch transverse size along the streak direction on the screen.

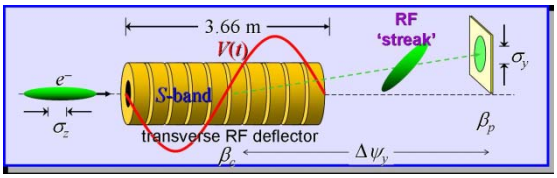

Figure 6: LOLA operation principle.

From (5) it is obvious that σ_y is not very sensitive to φ for small φ, but (4) shows that the centroid offset is then proportional to φ. For high resolution, the bunch should be streaked over a large fraction of the screen. The phase stability is then required to be significantly better than the phase length of the bunch: ≈0.1° for a bunch length of 25 µm and the 105 mm wavelength of the structure. Otherwise, the spot on the screen will jitter by more than the screen size.

Energy change due to beam loading from the LOLA structure within a bunch train is confined to approximately the first 80 bunches and amounts to no more than 0.03% [11].

REFERENCES

[1] B. Steffen, this conference (Paper ID TUPOS06)

[2] E.L. Saldin et al., DESY 04-126 (July 2004), also this conference (Paper ID THPOS65)

[3] J.S. Toll, Phys. Rev. **104**,1760 (1956)

[4] R. Lai, A.J. Sievers, Nucl. Instr. Meth. A397(1997) 221

[5] J. Menzel, private communication

[6] M. Dohlus, T. Limberg, Nucl. Instr. Meth. A407(1998) 278

[7] G. Geloni et al., DESY 03-031 (March 2003)

[8] S. Casalbuoni et al., EPAC '04, 5–9 July 2004, Lucerne, Switzerland (Paper ID THPLT046)

[9] M.A. Geitz, DESY-THESIS-1999-033 (November 1999)

[10] M. Nagel, FEL Report 2004 (to be published)

[11] K.L.F. Bane et al., SLAC-PUB-10160/TESLA Report 2003-24 (September 2003)